30 pages

October 1992

LU TP 92-25

Revisiting The Lund Fragmentation Model

B. Andersson[1], A. Nilsson[2]

Department of Theoretical Physics
University of Lund
Sölvegatan 14A
S-223 62 Lund, Sweden

Abstract

We present a new method to implement the Lund Model fragmentation distributions for multi-gluon situations. The method of Sjöstrand, implemented in the well-known Monte Carlo simulation program JETSET [1], is robust and direct and according to his findings there are no observable differences between different ways to implement his scheme. His method can be described as a space-time method because the breakup proper time plays a major role.

The method described in this paper is built on energy-momentum space methods. We make use of the x-curve, which is defined directly from the energy momentum vectors of the partons. We have shown that the x-curve describes the breakup properties and the final state energy momentum distributions in the mean [2].

We present a method to find the variations around the x-curve, which also implements the basic Lund Model fragmentation distributions (the area-law and the corresponding iterative cascade). We find differences when comparing the corresponding Monte Carlo implementation REVJET to the JETSET distributions inside the gluon jets.

[1] thepba@seldc52 (bitnet) bo@thep.lu.se (internet)
[2] thepan@seldc52 (bitnet) anders@thep.lu.se (internet)

1 Introduction

The Lund Model contains a set of basic concepts which cannot easily be changed without major inconsistencies in the model. Among these are that

- Quarks, q, and antiquarks, $\bar{q}$, are treated as excitations at the endpoints of the force field and gluons, g's, are internal excitations. The massless relativistic string is used as a (semi-classical) model for the force field. The above-mentioned excitations move like localised particles carrying energy momentum. They are acted upon by the string tension so that the q and $\bar{q}$ feels κ and the g's feel 2κ from the connected string pieces at rest.

- The original energy momentum of the partons is in this way transferred to the force field. The final state hadrons stem from the decay of the string along its space time history. Each breakup corresponds to the production of a new $(q\bar{q})$-pair. In the Lund Model this is done by means of a quantum mechanical tunnelling process in the force field. This process provides both for the relative flavor, transverse momentum and, at least qualitatively, for the particle production rates.

- The final state consists of a set of string pieces, in general yoyo-mode states, with a mass corresponding to a meson in the pseudoscalar and vector nonets (an extension to include tensor mesons is straightforward). There is also a mechanism, the popcorn mechanism, providing for baryon-antibaryon production at the level of around 10% of the meson production.

- For the particular case when there are no gluonic excitations, then the string field is stretched over a flat space-time surface. This surface is spanned between two lightcone directions, corresponding to the directions of motion of the q and $\bar{q}$ at the endpoints. In this case it is possible to show that there is a unique stochastic process for the breakup of the string.

- Apart from the regions in phase space close to the endpoints, the fragmentation regions, which each is of the order of $1 - 2$ units in rapidity, the process leads to an inclusively flat rapidity distribution for such a state.

- The surface spanned by the massless relativistic string is always a minimal surface. This means that all the properties of its interior is determined by the boundary. The boundary curve, which we will call the directrix, is in turn completely determined by the original excitations, ie by the partonic energy momenta.

  A second essential property of a minimal surface is that it is stable against small disturbances. In particular this means that the string space-time surface is *infrared stable*.

The breakup process on the flat surface can be generalised to a process on the more complex "bent" space-time surface, corresponding to multigluon states, under the particular assumption that a piece of a string can, if it fulfills the mass-shell condition, be projected onto a hadronic state with the same probability, irrespectively if it contains on the semi-classical level internal excitations or bends on the string.

Such a generalisation has been given by Sjöstrand [3]. We will provide a brief description of his method in the next section. There is in this generalisation a set of possible choices and it is shown in [3] that inside the scheme these differences do not lead to observable differences.

In this paper we will present a rather different approach to the fragmentation of a multigluon state. We will make use of the results in [2, 4], where it is shown that

- The directrix, which is built by the energy momenta of the original q, $\bar{q}$ and g's, corresponds to a space-time curve with an everywhere light-like tangent. It is possible to define a smooth time-like curve, which we will call the x-curve. The x-curve approximates the light-like directrix in the same way as a set of connected hyperbolas approximates the lightrays which corresponds to the asymptotes of the hyperbolas.

- The final state hadrons produced in the Lund Fragmentation Model, in accordance with the unique stochastic process and Sjöstrand's generalisation, will in an inclusive sense come out along the x-curve. In other words, in case we ask for the mean behaviour of the fragmentation process then we may partition the x-curve into pieces corresponding to the possible final state hadron masses.

In this way, the final state particles, produced along the x-curve, will contain energy momentum stemming from two or more adjacent original partons. By adjacent we mean color-connected in the same way as the color force field, modelled by the string, is stretched from the q via the internal g-excitations, ordered in color to the $\bar{q}$.

This is the Lund Model correspondence to the Local Parton Hadron Duality concept, brought up by the QCD theorists from the present St Petersburg [5].

We will in this paper define the fragmentation process as fluctuations around the x-curve. Compared to Sjöstrand's method, in which he all the time keeps to the string surface, in particular also when passing the gluon corners, our process moves close to the surface but not necessarily in the surface.

We feel that, as quantum mechanics does not really allow any precise localisation, this difference is of little interest. Both methods contains a local conservation of both flavor and energy momentum at each step of the decay process.

Using an intuitive picture one could say that Sjöstrand is using space-time notions along the string surface, while the method presented in here is based on energy-momentum space properties. In both cases semi-classical notions are used and none of the methods contain a full quantum mechanical treatment.

But it is never possible to implement any stochastical process in a practical way into a Monte Carlo simulation program without compromises. The way we do the fragmentation, which is conceptually very different from the well-known Sjöstrand Monte Carlo, JETSET, contains in this sense different compromises and therefore serves as a useful complement.

The method presented in here is also available as a Monte Carlo simulation program, REVJET [6], which is part of the Lund MC++ project [7]. All the comparisons are made between the JETSET and the REVJET Monte Carlo results in such a way that we have arranged the parameters so that the mean multiplicities of the events are the same.

Physically we find some interesting differences in particular for the properties of the particles inside the gluon jets. We find that the heavier particles in a gluon jet in general have larger momenta along the jet axis in REVJET than in JETSET. We also find systematic differences in the two-particle correlations.

The paper is organised in such a way that we present, in section 2, a brief account of Sjöstrand's method together with the necessary formalism to define the relationship between the directrix, the string surface and the x-curve. Then in section 3, we exhibit our method in some detail and we end in section 4 with some comparisons between the results of the two methods.

2 String Fragmentation a la Sjöstrand, the String Surface, the Directrix and the x-curve

2.1 The Relationship between the String Surface and the Directrix

In order to describe the string space-time surface we will consider a simple example of string motion. There will be a $(q, g, \bar{q})$-state, starting from a common origin with the q and $\bar{q}$ going out in opposite directions with the same energie, E, and the g will go transversely with the energy $E_2 < E$ (cf Fig 1).

Using a snapshot description at a few times the state will behave in the following way

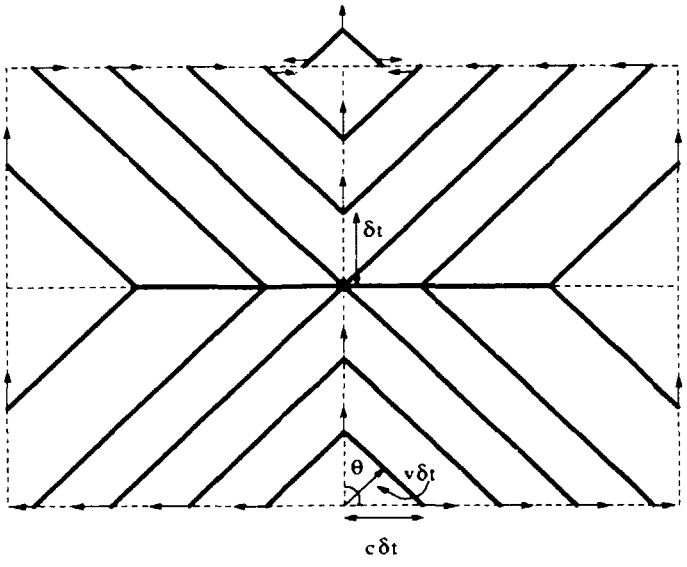

Figure 1: A half-cycle in the motion of a $(qg\bar{q})$-state as described in the main text

1. After a time δt the three partons have moved the distance δt along their directions and two field fronts have been created. The field fronts move upwards-outwards with the velocities $v = \cos(\theta)$ (transverse to the field fronts). The angle θ is for this configuration $\theta = \pi/4$ and is marked out in the figure. The size of the velocity is determined by the fact that the three partons all move with the velocity of light $c = 1$. The length of the wavefronts is $\delta l = 2\sin(\theta)\delta t = \sqrt{2}\delta t$.

   The front energies are $\kappa\delta l/\sqrt{1-v^2} = 2\kappa\delta t$. The corresponding longitudinal momenta are $\pm\kappa\delta l v\cos(\vartheta)/\sqrt{1-v^2} = \pm\kappa\delta t$ and the transverse momenta similarly $\kappa\delta t$ for each of the fronts.

   The q and the $\bar{q}$ has lost the energies $\kappa\delta t$ and the longitudinal momenta $\pm\kappa\delta t$, while the g has lost the energy and transverse momentum $2\kappa\delta t$. This means that the total energy momentum is accounted for. In the same way the remainder of the motion can be understood basically by local energy momentum conservation arguments.

2. This part of the motion continues until the g has lost its energy momentum, ie until $\delta t = E_2/(2\kappa)$. Then the $q\bar{q}$ continues outwards and a new segment is dragged out according to the Fig 1. The fronts follow outwards and serves as transporters of the energy momentum from the $q\bar{q}$ to the new segment. This motion continues until the $q\bar{q}$ has lost their energy momentum, ie until $\delta t = E/\kappa$.

3. After that the q and the $\bar{q}$ are dragged upwards by the wave fronts, absorbing

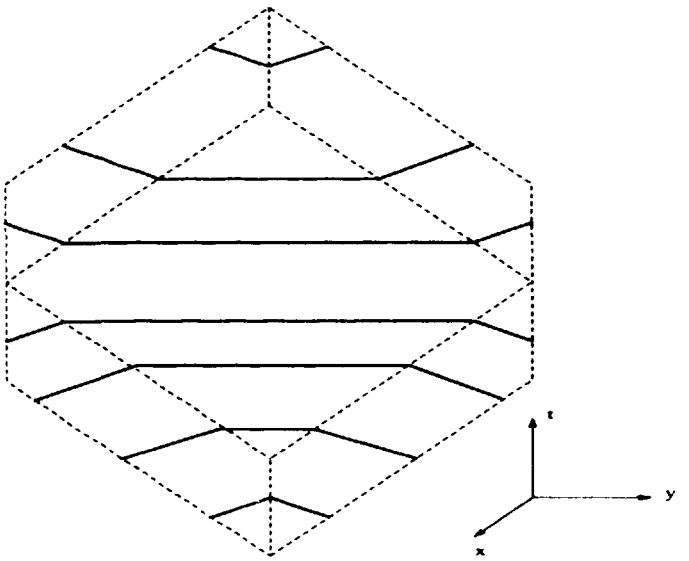

Figure 2: The space-time diagram of the motion described by the $(qg\bar{q})$-state

the energy momentum of the fronts until the time $(E + E_2/2)/\kappa$ when the string momentarily is at rest and the $q\bar{q}$ have the transverse energy momenta $E_2/(2\kappa)$.

4. After that the $q\bar{q}$ continue upwards creating two inward-moving fronts. After the further time $E_2/(2\kappa)$ they have lost all their energy momenta to the fronts. They start moving towards each other, dragged by the fronts, which transports energy momentum from the flat string piece in between back to the $q\bar{q}$.

5. After that the wave fronts meet and the g is recreated in the crossing of the wave fronts. Finally all three meet again, this time, however with the q and $\bar{q}$ moving in opposite directions to the starting situation.

   It will take another half-cycle of the string motion before they are back with the original states of motion. The time it takes for the full cycle is then $T = (4E + 2E_2)/\kappa$ and the meeting point after the full cycle is $\Delta = 2E_2/\kappa$.

It is a general property of the string motion that the full cycle takes the time $T = 2E_{tot}/\kappa$ and the string then moves $\vec{\Delta} = 2\vec{P}_{tot}/\kappa$. In Fig 2 the corresponding space-time diagram of the motion is depicted, with the string shown at some different times.

The most noticeable thing is that the original parton energy momenta completely determines the properties of the surface. Thus the right hand boundary curve (along which the q moves) can be described in turn by the energy momentum vector of the

q, k_q, of the g, k_g, and of the $\bar{q}$, $k_{\bar{q}}$. Similarly the $\bar{q}$-orbit is described in turn by $k_{\bar{q}}$, k_g, k_q. It is a general phenomena of string motion that anything the q does is done in the opposite order by the $\bar{q}$. We have used a scale such that $\kappa = 1$ in order to describe the space-time properties.

The whole thing clarifies if we define the four-vector valued function A. We will do it for a general string state containing n color-connected g's with energies e_j and energy momentum vectors k_j. The corresponding quantities for the q and $\bar{q}$ contain the indices 1 and $n+2$.

$$\begin{aligned}
A(\xi) &= k_1 \frac{\xi}{e_1}, \qquad 0 < \xi \leq e_1 \\
A(\xi) &= k_1 + k_2 \frac{(\xi - e_1)}{e_2}, \qquad e_1 < \xi \leq e_1 + e_2 \\
&\vdots \\
A(\xi) &= \sum_{j=1}^{n} k_j + k_{n+1} \frac{(\xi - \sum_1^n e_j)}{e_{n+1}}, \qquad \sum_1^n e_j < \xi \leq \sum_1^{n+1} e_j \qquad (1) \\
A(\xi) &= \sum_{j=1}^{n+1} k_j + k_{n+2} \frac{(\xi - \sum_1^{n+1} e_j)}{e_{n+2}}, \qquad \sum_1^{n+1} e_j < \xi \leq \sum_1^{n+2} e_j \\
A(\xi) &= A(\xi + 2E_{tot}) - 2P_{tot} \\
A(-\xi) &= -A(\xi)
\end{aligned}$$

The function A is the directrix and Eq (1) provides a general definition for an open string with excitations. The last line is specific for the case when the whole string passes through a single point.

We note immediately that the orbit of the q is given by $A(t)$, while the orbit of the $\bar{q}$ correspondingly is given by $(A(t + E_{tot}) + A(t - E_{tot}))/2$. The general motion for any point on the string is given by

$$x(t, \sigma) = \frac{A(t + \sigma) + A(t - \sigma)}{2} \qquad (2)$$

where σ is the energy in the string between the q-endpoint and the point parameterised by σ.

The description in Eq (2) can be understood as two forward and backward moving fronts along the string, containing a stream of energy grains. During the first part of the the motion there are according to Fig 2, grains leaving the q towards the $\bar{q}$. Together with the grains leaving the g towards the q, they form the right-moving front.

After that, the "original" q-grains form together with the $\bar{q}$-grains the flat string region between the two bends. The q absorbs half the g-grains (the rest goes towards

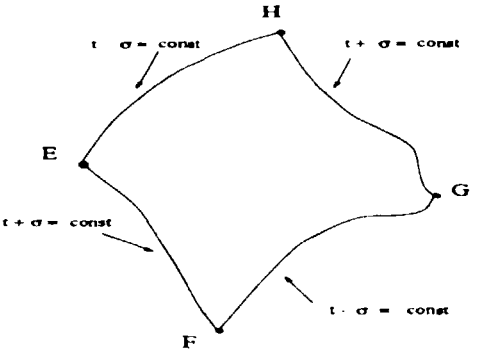

Figure 3: The causality diamond between the points $EFGH$ described in the main text.

the $\bar{q}$-side) and then emits them again. Together with the $\bar{q}$-grains they form the inwards moving front from the q-side. Finally the q absorbs the $\bar{q}$-grains.

It is of some interest to learn about the energy momentum content of different parts of the string. We first note, that the velocity vector, $\vec{v}_\perp$, is always transversely directed to the string direction while the tension, $\vec{T}$, in each point is along the tangent,

$$\begin{aligned} \vec{v}_\perp &= \frac{\partial \vec{x}}{\partial t} \\ \vec{T} &= \frac{\partial \vec{x}}{\partial \sigma} \end{aligned} \tag{3}$$

Furthermore the condition that the derivative of the directrix is always lightlike

$$\dot{A}^2(\xi) = 0 \Leftrightarrow |\dot{\vec{A}}(\xi)| = 1 \tag{4}$$

means that

$$\begin{aligned} \vec{v}_\perp \vec{T} &= 0 \\ \vec{v}_\perp^2 + \vec{T}^2 &= 1 \end{aligned} \tag{5}$$

We consider the causality diamond between the points $EFGH$, in Fig 3. This region is bounded by two curve-sets $t \pm \sigma = constant$ so that eg E and H has the same value of $t - \sigma$ and G and H the same value of $t + \sigma$. We obtain for the energy momentum floating across the EG equal-time line (using $d\vec{p} = d\sigma \vec{v}_\perp, de = d\sigma$):

$$\begin{aligned} P_{EG} &= \int_E^G d\sigma \frac{\partial x}{\partial t} \\ &= \int_E^G d\sigma \frac{\dot{A}(t+\sigma) + \dot{A}(t-\sigma)}{2} \\ &= \frac{A(+G) - A(+E) - A(-G) + A(-E)}{2} \equiv x(H) - x(F) \end{aligned} \tag{6}$$

In the same way we obtain for the energy momentum transfer across the line $\sigma = constant$ which joins FH:

$$P_{FH} = \int_F^H dt\vec{T} = \frac{A(+H) - A(+F) - A(-H) + A(-F)}{2} = x(G) - x(E) \qquad (7)$$

(there is no energy component in the last equation and we have used the notation $\pm G$ meaning $(t \pm \sigma)_G$ with eg $+G = +H$ etc).

The results can be generalised to the case when we consider the energy momentum content between two points on the string with a space-like difference. Then we obtain for the energy momentum floating across any space-like curve between them the difference vector between the corresponding tips of the causality diamond. Similarly the energy momentum passage along the string across any time-like curve joining two time-like points is given by the difference vector between the other two tips of the causality diamond.

2.2 The Unique Lund Fragmentation Process for a Flat String

A particularly simple example of string motion is provided by the case when there are no gluonic excitations and only an energy momentum carrying $(q\bar{q})$-pair at the endpoints. Then the lines $t \pm \sigma$ corresponds directly to the lightcone directions along which the q and $\bar{q}$ moves (cf Fig 4).

In this case it is possible to show that there is a unique process for the fragmentation of a string into final state hadrons with given masses. The general result for the (non-normalised) probability that the string breaks up into a n-particle final state is

$$dP_n = \prod_{j=1}^{n} N_j dp_j \delta(p_j^2 - m_j^2) \delta(\sum_{j=1}^{n} p_j - P_{tot}) \exp(-b\mathcal{A}) \qquad (8)$$

with $\mathcal{A}$ equal to the area spanned by the string before the breakup (shown in the figure as hatched). The formula contains a product of the phase space for the n particles together with the exponential area suppression.

There is one parameter, b, for the area suppression which is general for all kinds of particles. The relative probabilities N_j contains both flavor-, particle species and transverse momentum fluctuations.

The two terms generally compete so that in order to increase phase space one would like to make many particles. This is, however, countered by the area suppression and the compromise is that the particles tend to come out along a hyperbola. This means that there will be a basically flat rapidity distribution of the final state particles.

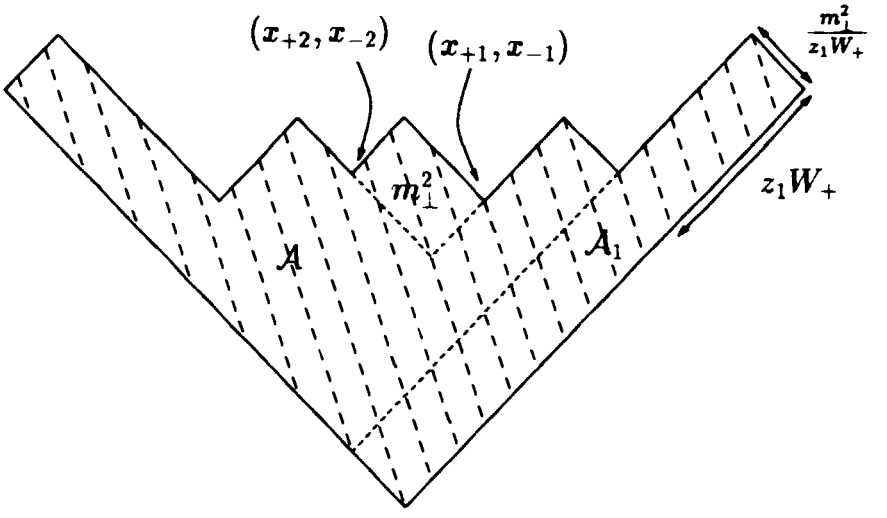

Figure 4: The breakup of as flat string with the total area, the area related to the first particle and also two vertices in the middle with a particle produced in between.

The expression in Eq (8) has very simple factorisation properties and this means that it is possible to subdivide it into an iterative cascade, where the particles are produced in a step-wise process. In case we sum over all n and integrate over all energy momenta we obtain a function of the only remaining Lorentz invariant, $P_{tot}^2 = s$,

$$\int \sum_n dP_n = g(s) \tag{9}$$

Furthermore if we rewrite dP_n into a term corresponding to the first particle and all the rest we obtain

$$dP_n(P_{tot}) = N_1 dp_1 \delta(p_1^2 - m_1^2) \exp(-b\mathcal{A}_1) dP_{n-1}(P_{tot} - p_1) \tag{10}$$

where the area $\mathcal{A}_1$ is the one marked out in the figure. If we integrate and sum over all the remainder but the first particle we obtain for the right hand side

$$N_1 \frac{dz_1}{z_1} \exp(-bm_{\perp 1}^2/z_1) g(s_1) \tag{11}$$

with $p_{1+} = z_1 W_+$ and $s_1 = (P_{tot} - p_1)^2 = (1 - z_1)(s - \frac{m_{\perp 1}^2}{z_1})$. We have here introduced the lightcone fraction z_1 and the transverse mass $m_{\perp 1}$ of the first particle and calculated the area $\mathcal{A}_1$ in the exponent and the mass-square of the remaining system s_1 in terms of them.

The result is an integral equation

$$g(s) = \int N_1 \frac{dz_1}{z_1} \exp(-bm_{\perp 1}^2/z_1) g((1 - z_1)(s - \frac{m_{\perp 1}^2}{z_1})) \tag{12}$$

which have asymptotic power-solutions $g(s) \propto s^a$ in case the power a fulfills

$$1 = \int N_1 \frac{dz_1(1-z_1)^a}{z_1} \exp(-bm_{\perp 1}^2/z_1) \tag{13}$$

This corresponds to an eigenvalue problem and it is possible to show that there is a unique value of a which fulfills the equation. From this we conclude that the inclusive distribution of the first particle will be

$$\begin{aligned} f(z_1)dz_1 &= N_1 \frac{dz_1}{z_1} \exp(-bm_{\perp 1}^2/z_1) \frac{g((1-z_1)(s-m_{\perp 1}^2/z_1))}{g(s)} \\ &= N_1 \frac{dz_1(1-z_1)^a}{z_1} \exp(-bm_{\perp 1}^2/z_1) \end{aligned} \tag{14}$$

It is possible to show that different flavors may correspond to different a-values. The corresponding generalisation of the fragmentation function $f_{\alpha\beta}$ is seldom used in the Lund Model,

$$f_{\alpha\beta}dz = N_{\alpha\beta} \frac{dz(1-z)^{a_\beta}}{z} z^{a_\alpha - a_\beta} \exp(-bm_\perp^2/z) \tag{15}$$

The indices are such that we go from a vertex with flavor α towards a vertex with flavor β with the production of the particle. We will use this form in connection with heavy quark fragmentation.

The distribution f is used in both the simple $(q\bar{q})$-situation and in Sjöstrand's generalisation as well as the one presented in here. It has the unique property that it does not matter whether the fragmentation is done in one or the other directions along the string. It is completely symmetrical and it can even be proved that in case the string is subdivided into similar subsystems then each of them can be fragmented in the same way independent of the others.

One such subdivision is provided eg by concentrating upon a single breakup space-time point, which we will call a vertex (cf Fig 4 where two adjacent vertices are marked out with the space-time coordinates (x_{+j}, x_{-j}). Any such vertex subdivides the event into two parts, the final state particles which move "to the left" (ie towards the $\bar{q}$-end) and those moving to the right.

We will make two comments on these vertices,which we will need later:

V1 The total energy momentum content of the particle jet which moves towards the q end with respect to the vertex, with index 1, is $(W_+ - \kappa x_{+1}, \kappa x_{-1})$. Similarly the energy momentum content of the jet moving towards the $\bar{q}$-end is $(\kappa x_{+1}, W_- - \kappa x_{-1})$. Then it is possible to describe the situation in terms of the diagram in Fig 5.

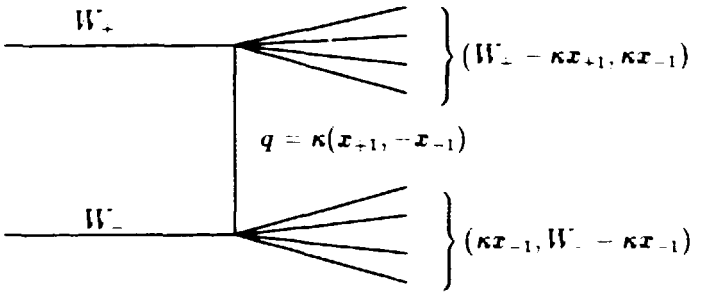

Figure 5: A multiperipheral ladder diagram with the momentum transfers corresponding to the vertices in the space time breakup of the Lund String.

The two original partons come in, the q with W_+ and the $\bar{q}$ with W_-, have an energy momentum transfer (from q towards $\bar{q}$) of $\kappa(x_{+1}, -x_{-1})$ and emerge as the two final jets. Actually all the vertices in space-time can in this dual language be described as such energy momentum transfers.

In this way the Lund Model appears as a multiperipheral kind of model. The factorisation properties and the ensuing integral equations are all similar to the use of multiperipheral results in the unitarity equations of the S-matrix. In this language the parameter a derived above would be a Regge-intercept parameter.

The dual relationship between the vertex positions and the momentum transfers is of course the same relationship as we exhibited at the end of the last subsection on the energy-momentum transfer across two points with a timelike connection.

V2 We assume that the particle with transverse mass $m_\perp$, which is produced in between the vertices 1 and 2 in Fig 4 takes the positive lightcone fraction z of the remaining energy momentum. That means $\kappa(x_{+1} - x_{+2}) = z\kappa x_{+1}$. Then we obtain immediately for the relationship between the two proper-time-variables (or squared momentum-transfers) $\Gamma_j = \kappa^2 x_{+j} x_{-j}$ that

$$\Gamma_2 = (1 - z)(\Gamma_1 + \frac{m_\perp^2}{z}) \tag{16}$$

Inside the same approach as when the symmetric Lund fragmentation function f was derived it is possible to show that there is a unique distribution $H(\Gamma)$ with the property that

$$H(\Gamma_2) = \int dz f(z) H(\Gamma_1) d\Gamma_1 \delta(\Gamma_2 - (1 - z)(\Gamma_1 + \frac{m_\perp^2}{z})) \tag{17}$$

which is

$$H(\Gamma) = C\Gamma^a \exp(-b\Gamma) \tag{18}$$

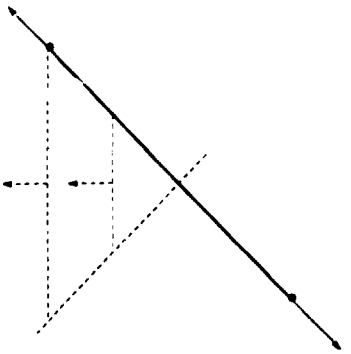

Figure 6: The segment (qg) shown in the rest-frame, where they go apart with the velocity of light.

The two relations in Eqs (18) and (16) provides the inclusive Γ-distribution and the correlation between two adjacent Γ's.

2.3 Sjöstrand's Method to Fragment Multigluon Strings

In case we would boost to the restframe of one of the two fronts which is spanned between the qg or $g\bar{q}$ in the $(qg\bar{q})$-state shown in Fig 1 then we obtain Fig 6. The q and the g goes apart in opposite directions and there is no real differences between the q-region in this case and in the case discussed in the last subsection.

The same would be the case for the region adjacent to the $\bar{q}$ in the restframe of the $g\bar{q}$-segment. We note, however, that there are some problems to continue the space time discussion too close to the g corner.

To see the problem assume that there is a $q_1\bar{q}_1$-pair produced along the qg-segment. Then the string piece between the $q\bar{q}_1$ is just an ordinary flat string and we may use the methods of the last section. For the newly produced q_1 a continuation of the classical motion will, however not lead to a simple result. The q_1 will be dragged upwards by the remaining front and actually go out of the original string surface.

There are other problems also related to the fact that a break around a g-corner does no longer bring back a system of the same kind as we started with. The way Sjöstrand approaches the fragmentation is then to consider the space-time surface of the original parton state as "frozen" and to apply the stochastic string fragmentation process as a process in this surface.

Thus one considers the partonic state as a quantum state and the ensuing string

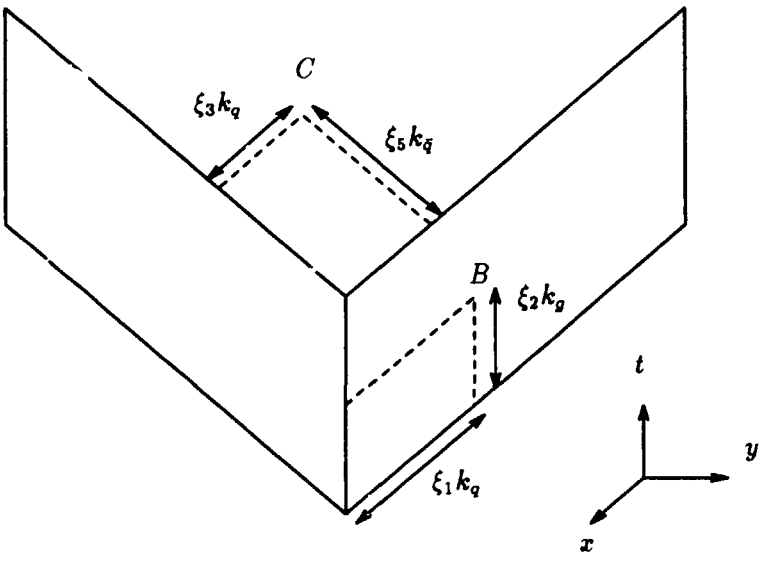

Figure 7: A few points are shown along the string surface with their coordinates as described in the text.

surface with its directrix as a description of the state in connection with the decay process. We will in this paper use the same interpretation.

The general idea in Sjöstrand's method is to generalise the proper time notion to an arbitrary point along the string space-time history. In Fig 7 we show the space-time surface of the $(qg\bar{q})$-state again, with a few points marked out. We note that any point inside the front regions, like eg the point B is of the same character as the flat field case we discussed in the last sub-section. The point B can be described in terms of the coordinates

$$B = \xi_1 k_q + \xi_2 k_g \Rightarrow \Gamma_B = \xi_1 \xi_2 s_{qg} \tag{19}$$

with s_{qg} the mass of the two index partons.

For the point C there is a corresponding coordinate description, but this time containing all three parton vectors:

$$C = \xi_3 k_q + \xi_4 k_g + \xi_5 k_{\bar{q}} \tag{20}$$

The proper time variable Γ_C can be described in terms of these coordinates and the sub-masses of the partons. The coordinate $\xi_4 = 1/2$ in this case. It is easy to convince oneself that any point on the string surface has such a coordinate description with some constraints.

It is also possible to calculate the energy momentum, which floats between B and C. We may then use the results of Eq (6) or directly the coordinates shown in Fig 7.

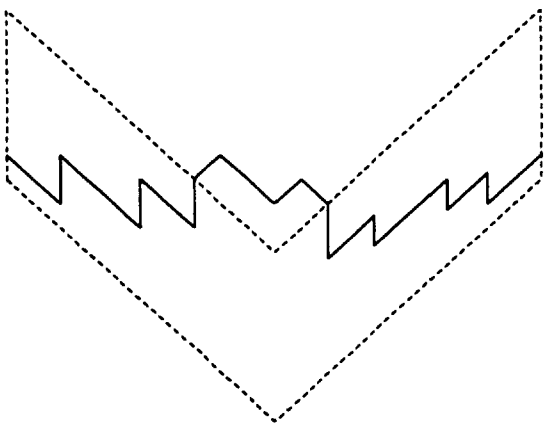

Figure 8: The breakup of the string along two hyperbolas in the front regions and some particles around the gluon corner.

The result for the energy momentum is

$$P_{BC} = (\xi_1 - \xi_3)k_q + (1/2 - \xi_2)k_g + \xi_5 k_{\bar{q}} \tag{21}$$

We assume that in the cascade we have reached the point B (ie we know the coordinates ξ_1 and ξ_2). Then we would like to produce a particle with a given squared mass $m_{BC}^2 = P_{BC}^2$ by a step to the point with a given $\Gamma = \Gamma_C$. From the equations we find two unknown coordinates (ξ_3, ξ_5). The two equations, corresponding to the cutting point of two hyperbolas, then provide a precise answer for the point C.

Sjöstrand then uses the relation in Eq (16) in order to obtain the value Γ_C, knowing the value Γ_B. He chooses all the time the parameter z by means of the symmetric Lund fragmentation function f with the right mass inserted.

His procedure is exact as long as he is producing points in simple regions containing only two lightcone directions (flat string segments) and provides a well-defined way to go around the gluon corners as we have shown above. The method is, however, not unique because the parameter z does not have a precise meaning, as eg the remaining energy momentum fraction, in connection with the corners.

Using his method we would obtain as a typical breakup situation the two yoyo-hadron regions close to two hyperbolas which are exhibited in Fig 8. The invariant length of a hyperbola corresponding to the mass square s is $\simeq \log(s/s_0)$ and the corresponding length is in this case $\simeq \log(s_{qg}/s_0) + \log(s_{g\bar{q}}/s_0)$.

It is easy to generalise the result to a multigluon state like the one we discussed in connection with Eq (1). Using the same notations we expect a generalised phase

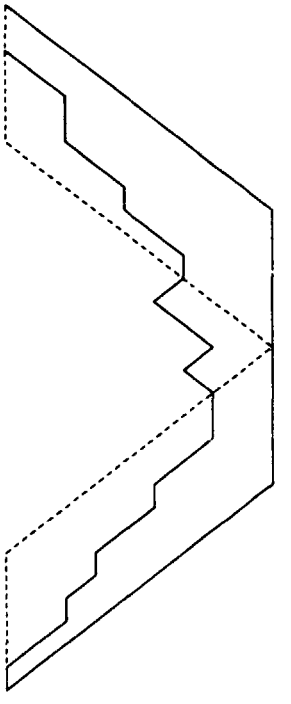

Figure 9: The particles produced in connection with the fragmentation in space-time are redrawn along the directrix.

space length, corresponding to $(n+1)$ hyperbolas

$$\lambda_n = \sum_{j=1}^{n+1} \log(s_{jj+1}/s_0) \tag{22}$$

It turns out that the quantity λ_n is a very good measure of the final state particle multiplicity with the two requirements

$\lambda 1$: It is necessary to make a suitable choice of the scale s_0.

$\lambda 2$: It is necessary to stop the partonic cascade such that all mass squares between adjacent partons is above s_0.

In the next section we will extend this result to an infrared stable definition of the quantity λ.

2.4 The x-curve and an Infrared Stable λ-Measure

In order to understand the idea behind the x-curve, consider Fig 9. In this picture the yoyo-hadrons, which are produced around the two hyperbolas in Fig 8, are drawn instead as hyperbolas spanned along the directrix. It is of course the same hadrons but while their production points are emphasized in Fig 8 it is instead their energy momentum vectors which play the role of connectors in Fig 9. The curve exhibited in this way is essentially the x-curve.

For a mathematical description we define a functional $T(\xi) \equiv \exp(\lambda)$ and a vector $q(\xi)$ along the directrix A by means of the differential equations

$$\begin{aligned} dT &= \frac{(qdA)T}{m_0^2} \\ dq &= dA - \frac{(qdA)q}{m_0^2} \end{aligned} \tag{23}$$

For the vector q we obtain formally, with the boundary value $q(\xi = 0) = 0$ that

$$q(\xi) = \frac{1}{T(\xi)} \int_0^\xi dA(\xi')T(\xi') \tag{24}$$

Thus q is a weighted mean of the partonic energy momentum vectors as described by the directrix. Similarly we obtain for T with the boundary value $T(\xi = 0) = 1$:

$$T(\xi) = \exp\left(\frac{1}{m_0^2} \int_0^\xi q(\xi')dA(\xi')\right) \tag{25}$$

This means that T is the exponent of an area because the area element spanned by the vectors q and dA is $d\Sigma = \sqrt{(qdA)^2 - q^2dA^2} = qdA$. If we multiply the second line of Eq (23) with q we also find that

$$dq^2 = 2(1 - \frac{q^2}{m_0^2})qdA \Rightarrow q^2(\xi) = m_0^2(1 - T^{-2}(\xi)) \tag{26}$$

Thus q becomes time-like and its invariant length quickly approaches the value m_0.

If we introduce the case when the directrix is built up by the finite light-like parton energy momentum vectors as in Eq (1), then we can construct the quantities T and q recursively by

$$\begin{aligned} T_{j+1} &= \frac{T_j}{\gamma_{j+1}} \\ q_{j+1} &= \gamma_{j+1}q_j + \frac{1}{2}(1 + \gamma_{j+1})k_{j+1} \\ \gamma_{j+1} &= \frac{1}{1 + (q_jk_{j+1})/m_0^2} \end{aligned} \tag{27}$$

We note that in this way

$$\begin{aligned} q_0 &= 0 \\ q_1 &= k_1 \\ q_2 &= k_2/2 + (k_1 + k_2/2)/(1 + k_1 k_2/m_0^2) \simeq k_2/2 \end{aligned} \tag{28}$$

etc. Similarly for T we have

$$\begin{aligned} T_0 &= 1 \\ T_1 &= 1 + \frac{s_{12}}{2m_0^2} \\ T_2 &= 1 + 2(\frac{s_{123}}{4m_0^2} + \frac{s_{12}s_{23}}{16m_0^4}) \end{aligned} \tag{29}$$

etc. The highest power in T always has the generic form

$$2\frac{s_{12}}{4m_0^2}\frac{s_{23}}{4m_0^2}\cdots\frac{s_{n+1,n+2}}{4m_0^2} \tag{30}$$

This means that

T1: In general $\log(T)$ is a good approximation to the quantity λ, defined in the last section.

T2: In case any of the partons become collinear or soft then the next order term in T will take over so that λ, defined in this way, is infrared stable.

T3: The result in Eq (25) that $\log(T)$ is the area between the x-curve and the directrix provides an intuitive understanding of the relationship between the fragmentation process and the partonic state as described by the directrix.

It is possible to find a solution for the vector q, which we will call $\hat{q}$ which is periodic in the same sense as the directrix is periodic. For the case above this means that $\hat{q}_j = \hat{q}_{j+2(n+2)}$. In this case $\hat{q}^2 = m_0^2$. The vector $\hat{q}$ can to a good approximation be constructed by iterating Eqs (27) a few periods around the string directrix.

We will from now on only work with this periodic q-vector and therefore we drop the hat-notation. The x-curve is then defined in terms of this periodic q as

$$x(\xi) = A(\xi) - q(\xi) \tag{31}$$

From this result we obtain that the vector q is the tangent of the x-curve in every point with a length such that it reaches from the x-curve to the directrix:

$$dx(\xi) = dA(\xi) - dq(\xi) = \frac{qdA}{m_0^2}q \tag{32}$$

Finally it is possible to do exactly the same construction as we have done from the q-end also from the $\bar{q}$-end and to define the corresponding q-vector and x-curve in that case.

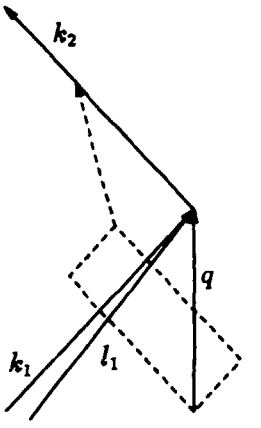

Figure 10: The situation in the restframe of the q-vector with the "new" k-vector, k_2, and the vectors $k_1 \simeq l_1$. The first fragmentation step is marked out together with the "new" q-vector along the handrail directrix.

3 The Method to Fragment Along the x-Curve

3.1 The Ordinary Case with Light Flavors

We note that the x-curve is basically obtained by a motion in each segment (k_j, k_{j+1}) such that there is a tangent vector q, with fixed invariant length, which connects to the directrix like "an arm on a handrail". This is the way we are going to fragment along the x-curve. We start on the curve and then take "steps" in a generalised segment, determined by the curve and the directrix, but all the time keeping the arm on the handrail, ie the directrix.

To see the procedure in detail consider the situation in the restframe of the vector q_1, obtained as the periodic solution after we have passed k_1 (cf Fig 10). We have in the figure exhibited both q_1, k_1 and k_2. We will then from the vectors q_1 and k_2 construct another light-like vector l_1 in the plane of these two,

$$l_1 = 2q_1 - \frac{\gamma_1}{(1-\gamma_1)} k_2 \tag{33}$$

where we have used the notation γ_j from Eq (27). The factor 2 on the q-vector can be understood from the Eq (28). In general the vector l_1 is close to the vector k_1.

The basic idea is now to fragment the state defined by (l_1, k_2) as if we were fragmenting a flat string segment.

We assume that we know the flavor of the endpoint q (for the moment we assume that

it is a light-mass flavor, which can be treated as massless). Then we use the same ideas as in JETSET to produce a new flavor, transverse momentum (cf below) and thereby the first rank hadron from the q-side. (We will use superscripts to describe rank and subscripts to describe the steps along the directrix).

Then we use the Lund fragmentation function f, with the correct (transverse) mass, to produce a fractional energy momentum along the defined l_1-direction, $z^{(1)}l_1$. In order to reconstruct the transverse mass, $m_\perp^{(i)}$ we assume that the corresponding fraction of k_2, $z'^{(1)}k_2$, making up the first rank particle energy momentum, $p^{(1)}$, fulfills

$$\begin{aligned} p^{(1)} &= \frac{1}{2}(z^{(1)}l_1 + z'^{(1)}k_2) \\ (p^{(1)})^2 &= \frac{1}{2}z^{(1)}z'^{(1)}l_1k_2 = (m_\perp^{(1)})^2 \end{aligned} \tag{34}$$

We next construct a new q-vector by choosing $q_1^{(1)}$ (the q-vector after the first rank particle has been produced) such that

$$\begin{aligned} q_1^{(1)} &= q_1 - p^{(1)} + \alpha^{(1)}k_2 \\ (q_1^{(1)})^2 &= m_0^2 \end{aligned} \tag{35}$$

which fixes $\alpha^{(1)}$.

After the first step we will be in one of three possible situations:

S1 either the calculated quantities

$$\begin{aligned} z'^{(1)} &\leq 2 \\ \alpha^{(1)} &\leq 1 \end{aligned} \tag{36}$$

S2 or

$$\alpha^{(1)} > 1 \tag{37}$$

S3 or

$$z'^{(1)} > 2 \tag{38}$$

For the case S1 we just repeat the procedure and produce a second rank particle etc.

For the case S2 we have taken a step which is larger than we are supposed to do with respect to the "handrail". There is then a new vector k_3, corresponding to the next color-ordered gluon and we will just continue along that vector with the handrail.

This means that we calculate the number $\alpha_2^{(1)}$ by

$$\begin{aligned} q_2^{(1)} &= q_1 - p^{(1)} + k_2 + \alpha_2^{(1)} k_3 \\ (q_2^{(1)})^2 &= m_0^2 \end{aligned} \tag{39}$$

If necessary we continue "upwards" along the directrix in an obvious way. These situations do not occur very frequently but in case the partonic cascade is continued down to small invariant masses then there may be many soft gluons, which will be "passed over" by the procedure.

In the case S3 we have taken a step which is larger than we are supposed to do with respect to energy momentum conservation. In that case we go back to the place we were before the step. Then we define from that point a new q-vector, $q_2^{(1)}$ by means of

$$\begin{aligned} q_2^{(1)} &= q_1 + k_2 - \alpha_2^{(1)} k_3 \\ (q_2^{(1)})^2 &= m_0^2 \end{aligned} \tag{40}$$

After that we construct a new l-vector, l_2 by the same procedure as before (Eq (33)) from $(q_2^{(1)}, (1 + \alpha_2^{(1)})k_3)$. Then we take the already defined step z along this vector, define z' by

$$\begin{aligned} p^{(1)} &= \frac{1}{2}(z l_2 + z' k_3) \\ (p^{(1)})^2 &= m_\perp^2 \end{aligned} \tag{41}$$

and continue.

This case does not occur except when the first gluon vector, k_2, is essentially collinear to the q energy momentum vector k_1 so that there is little energy momentum in the first string segment (k_1, k_2).

The adjustment when the energy momentum is not sufficient is not a unique prescription but we have not seen any traces of the procedure in the final state observables. It is also manifestly infrared stable.

The formulas written above for the cases S2 or S3 are valid in case the problem occurs already in the first step. If we have already taken a set of steps, thereby using up some parts of "the handrail" then the vector $k \to (1 - \sum \alpha_j)k$ in the formulas above.

There are two further necessary parts to be defined in our method. The first is the transverse momentum generation. This is done along the same lines as for JETSET, ie we chose at every step with a gaussian distribution a transverse vector $\vec{k}$ and give to the produced $(q\bar{q})$-pair, $\pm\vec{k}$, respectively. The transverse momentum of the final hadron is obtained as the vector sum of the one from the constituent q and $\bar{q}$.

"Transverse" is then defined as transverse with respect to the space-direction spanned by the relevant (k,l)-combination at every step. When we pass a gluon corner the 'old' transverse momentum is not necessarily transverse with respect to the new (k,l)-combination. This is handled in the following way.

First we transform $p_\perp \equiv (0,p_x,p_y,0)$ to the system where the new (k,l)-pair goes back to back along the z-axis. Then we write the new $p_\perp$ as a sum of three pieces

$$p_\perp \equiv (p_{\perp e},p_{\perp x},p_{\perp y},p_{\perp z}) = (0,p_{\perp x},p_{\perp y},0) + (p_{\perp e},0,0,p_{\perp e}) + (0,0,0,p_{\perp z}-p_{\perp e}) \quad (42)$$

The first term is the new transverse momentum. The second ($\equiv e_{\rm corr}$) and the third ($\equiv z_{\rm corr}$) terms are then corrected for in the following way. We change $l \rightarrow l - e_{\rm corr}$. Then we take the ordinary step with the right transverse mass, ie we define a particle with a certain momentum, p, along the z-axis. The momentum of this particles is changed $p \rightarrow p - z_{\rm corr}$ and the energy is changed in order to keep the particle on mass-shell. This means in general a small change in the chosen fragmentation variable.

There is also the method of how to end the cascade. We have also here used the same method as in JETSET. We take a step either from the q- or from the $\bar{q}$-end with equal probability. This means that we are after every fragmentation step left with a certain total remaining mass of the state.

When this mass passes under a certain threshold mass, we then produce a final two-particle state with flavor, transverse momentum and particle type in accordance with the ordinary Lund probabilities. There are in general two solutions to the kinematical equations and we have chosen them with an equal probability. This leads to an in general flat rapidity distribution in the case of a simple $(q\bar{q})$-string fragmentation.

There is in our method a parameter m_0. This parameter determines the resolution of the partonic state in connection with the fragmentation. There is another such parameter, which is directly linked to the end of the partonic cascade. In ARIADNE [8], which implements the Dipole Cascade Model [9], this parameter is the smallest allowed transverse momentum $k_{\perp cut}$.

In case m_0 is chosen essentially above $k_{\perp cut}$ then several gluons may in general be passed in a single step along the handrail-directrix. We have therefore in general kept $m_0 \simeq 0.3 - 0.4\ GeV$ in the results reported in here, ie in general a bit below the cascade cutoff. The results are not sensitive to the precise value we use for m_0 (although we may have to make minor adjustments to the fragmentation parameters (a,b) in order to keep to the same multiplicity, cf below).

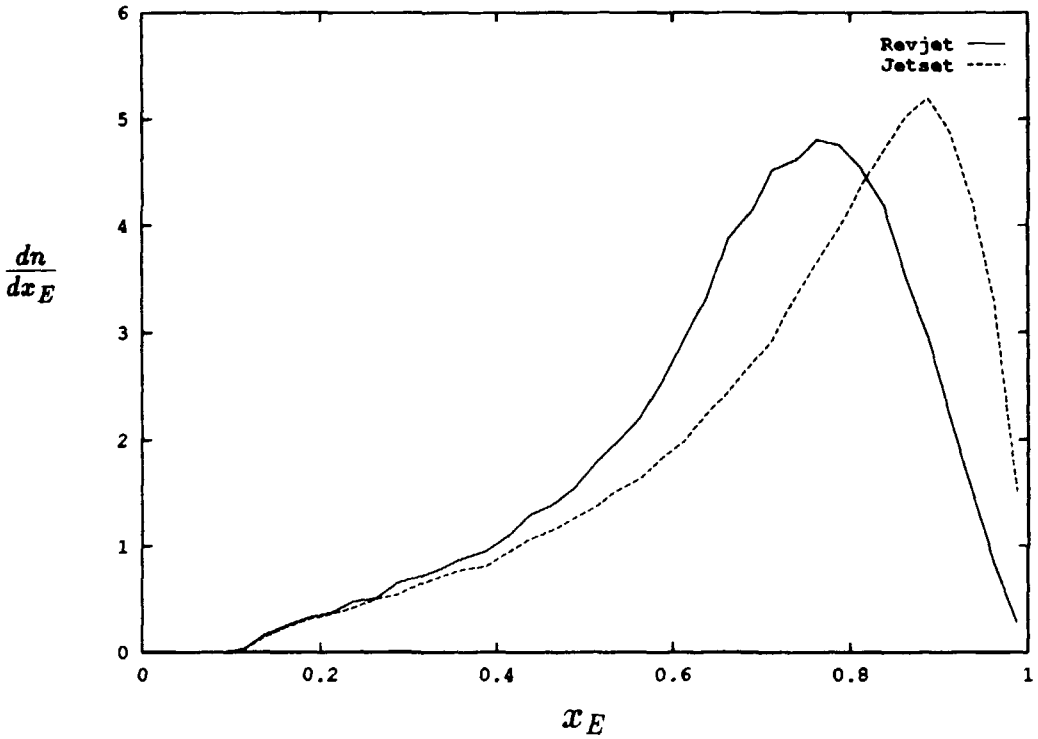

Figure 11: The distribution of bottom mesons in JETSET and REVJET.

3.2 Heavy Flavor Fragmentation

According to the Lund Tunneling Scenario, in which the main parameter is the string tension $\kappa \simeq 1\ GeV/fm$, the production of $u : d : s$-flavors is chosen as $3 : 3 : 1$. The tunneling formula, predicting the probability to produce a flavor corresponding to mass μ behaves as $\simeq \exp(-\pi\mu^2/\kappa)$. It would not allow production of the c-flavor at a larger rate than 10^{-9} and the b-flavor at an astronomically small rate.

These flavors may, however, occur at the endpoints of a string, if they are produced by the hard partonic cascade. In connection with our definition of the directrix it is difficult to accommodate heavy flavors. They would not move along lightcones but along hyperbolas which have the corresponding lightcones as asymptotes. It is then necessary to take such corrections into account.

There has been a suggestion by Bowler [10], that for an area suppression law there will be an appreciable correction from the hyperbola motion of the heavy flavor. The

exponential factor in the fragmentation function f in Eq (14) is changed so that

$$\frac{m^2}{z} \rightarrow \frac{m^2}{z} - \mu^2 \log\left(1 + \log\left(\frac{M^2}{\mu^2 z}\right)\right) \tag{43}$$

Therefore if we introduce this area in the definition of f we obtain the particular shape

$$f_B = \frac{N' dz}{z} z^{(a_i - a)}(1-z)^a \exp - \frac{bM^2}{z} \tag{44}$$

This is the distribution in Eq (15) with

$$a_a \equiv a_i = a - b\mu^2 \tag{45}$$

This means that the first a-parameter value should be diminished in a heavy quark jet. Besides that we do not need to worry more about the fact that this first flavor is heavy. We can use the traditional way to remake a massive q or/and $\bar{q}$ into a massless one [3], and then apply this fragmentation function.

The result is that the prescription in JETSET for heavy quark fragmentation actually will be changed appreciably *but the prescription is perfectly allowed in the Lund Model.* The derivation of the fragmentation function [11], works just as well. The result is a softer fragmentation function.

The distribution of bottom hadrons is changed very much in our approach compared to JETSET. In Fig 11 we show the distributions for the two cases.

For the charmed mesons there are two contributions, one from directly produced D^*'s from charm-jets and one from the decay of B-mesons. Taken together there is a rather small difference between JETSET, our prediction and the data. It is, however, probably possible inside the very large statistics from the LEP-experiments to trigger on a semi-leptonic decay of one of the $(b, \bar{b})$ or $(c\bar{c})$ and investigate the fragmentation of the other.

4 Comparisons Between JETSET and The Method in This Paper

There are three major parameters both in JETSET and in REVJET, although REVJET also contains an extra parameter m_0. As we have said before m_0 is chosen to be smaller than the cutoff in the partonic cascade and then there are no traces of it. If it is chosen differently then it is in our experience always possible to change the b-parameter correspondingly so that m_0 is really no new degree of freedom.

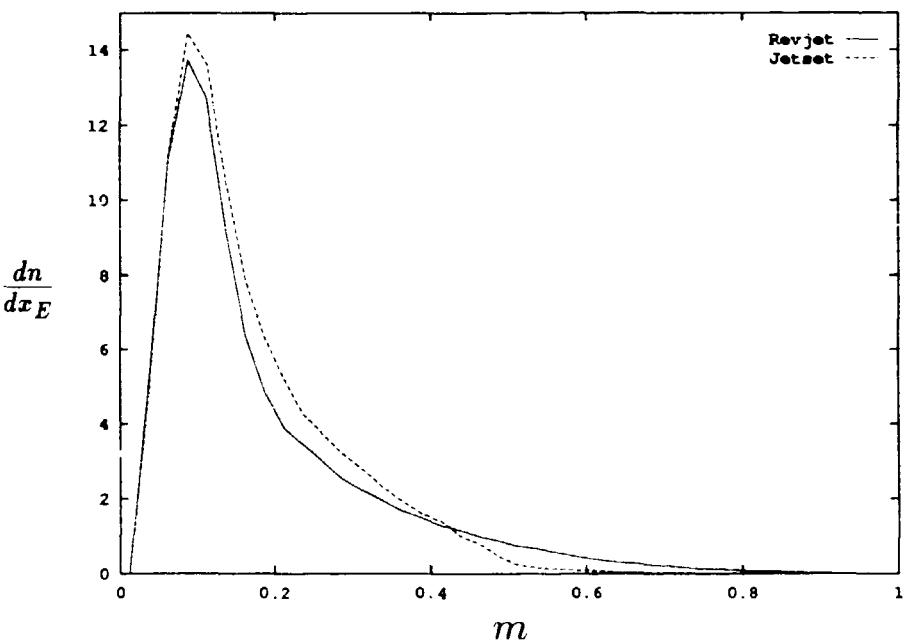

Figure 12: The distributions of baryons inside a gluon jet, defined in accordance with the text.

We have chosen the same default values in REVJET as in JETSET for the parameter σ, the width of the gaussian transverse momentum. We have also, besides the heavy quark fragmentation in the last section, chosen the same default value for the a-parameter in the fragmentation function. For all the comparisons below we have then arranged the b-parameter in such a way that we obtain the same mean total multiplicity in JETSET and REVJET.

The general result is that every inclusive single particle distribution coincide between the JETSET and the REVJET simulations, at least outside of the gluon jets. In connection with the gluon jets there is a systematic difference between the results of the two methods. The heavy particles will in our method in general be faster along the gluon jet axis than in JETSET. There is, however basically no difference between the pions and kaons in the two methods.

In Figs 12 and 13 we show the results of a comparison in connection with a 50 GeV gluon jet. We have plotted the x_E-distributions for all particles inside a cone of the size ± 0.75 in rapidity around the gluon jet. The jet has not been developed further by a partonic cascade. It means, however, that we tend to obtain a smaller total multiplicity in a gluon jet, although it is a small effect.

There is an interesting systematics between the behaviour of the b-parameter in the

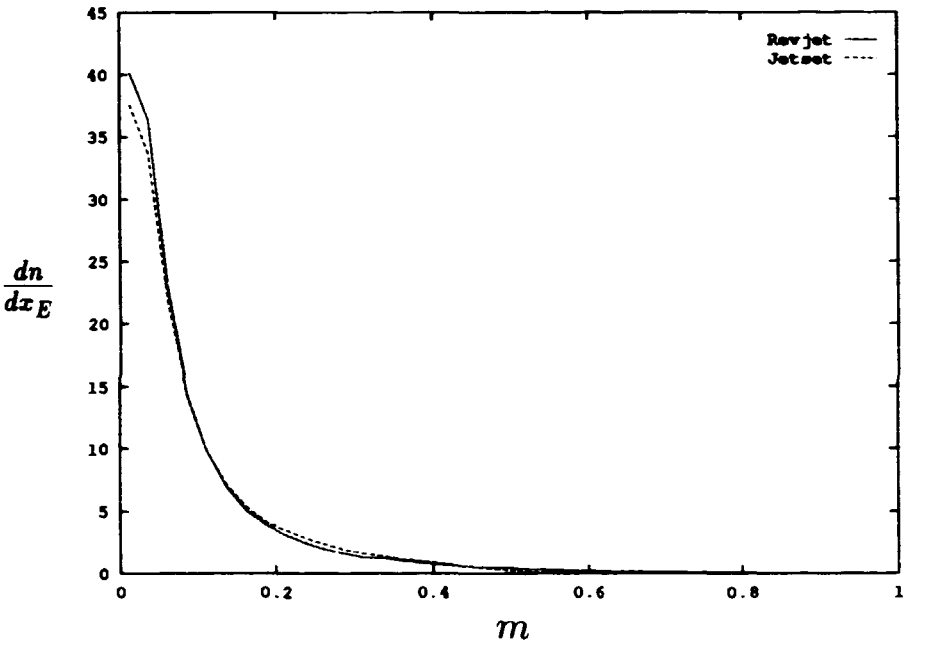

Figure 13: The distributions of pions inside a gluon jet.

two methods. In [12] it was pointed out that there is a moving interface in the Lund Model between the partonic cascades and the fragmentation.

It is possible to obtain essentially the same final state hadron distributions in case we stopped an ARIADNE [8] cascade at a value $k_{\perp cut} = 7\ GeV$ or any value down to above the Λ_{QCD} if we chose the b-parameter accordingly. (There was no need to change the a- and σ-parameters according to the findings in [12]). In Fig 14 we show the corresponding values of b needed for JETSET and for REVJET. It is noticeable that while the b-parameter changes appreciably for JETSET there is actually a rather small change for REVJET.

From the expression for f it is obvious that a larger value of b corresponds to a larger value of the fragmentation parameter z and therefore to a use of more energy momentum in the string in every step. Correspondingly the value of Γ in Sjöstrand's method decreases. This is necessary for a multi-gluon string surface which will occur for small $k_\perp$-cutoffs.

Sjöstrand's method all the time keeps to the string surface. The method in this paper will in general get more easily around the many small gluon corners because it will basically pass over the corners and continue wherever it is possible. A string containing many small gluons will in this way be "smoothed out" by the method presented in here.

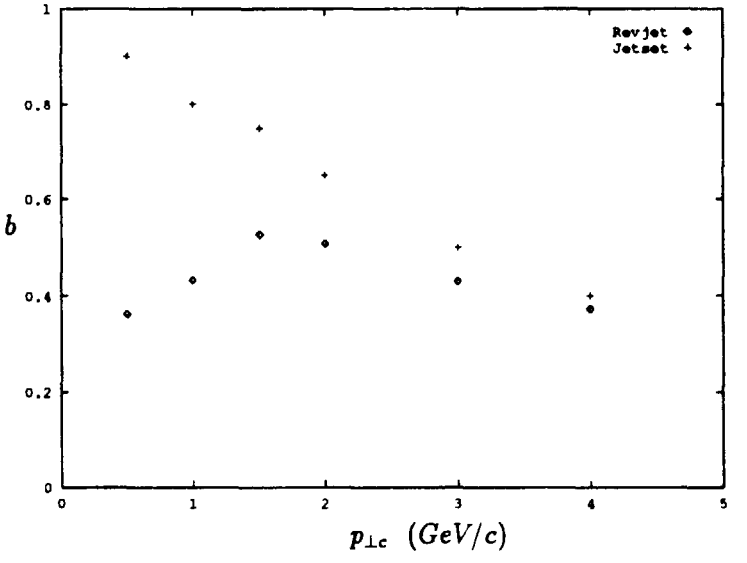

Figure 14: A comparison between the b-parameter needed in JETSET and REVJET to describe the same physics in multigluon events.

The third place where we have found differences is in connection with the two-particle correlations in the gluon jets. We have investigated in detail some simple gluon configurations, in particular the case when we have a q and $\bar{q}$ going out in opposite directions with energies W_q. There will be two gluon jets with energies W_g going in the same azimuthal angle and symmetrically with the angles θ_g with respect to the q- and $\bar{q}$-directions. We have also investigated different other configurations but these ones bring out the main features.

We have defined the following regions in phase-space. Each gluon jet is defined by means of a cone around the jet corresponding to the size $\pm.75$ in rapidity. There is also a forward (backward) q ($\bar{q}$) fragmentation region and finally, in case the angle $\pi - 2\theta_g$ is sufficiently large, also a central region. Independently of the angles and the gluon energies there are no differences in the two-particle correlations in the forward, backward and central regions.

We have defined the two-particle correlations in the following way. We generate one first event and consider the combined mass-distribution of all the relevant pairs. Then we generate a second event and produce the same distribution from one particle in the first and one in the second event. Then the procedure is repeated with the second event taking the place of the first. We normalise the same event sample to $\langle n^2 \rangle$ and the mixed event sample to $\langle n \rangle^2$ and present the ratio of the sample as a function of the combined mass.

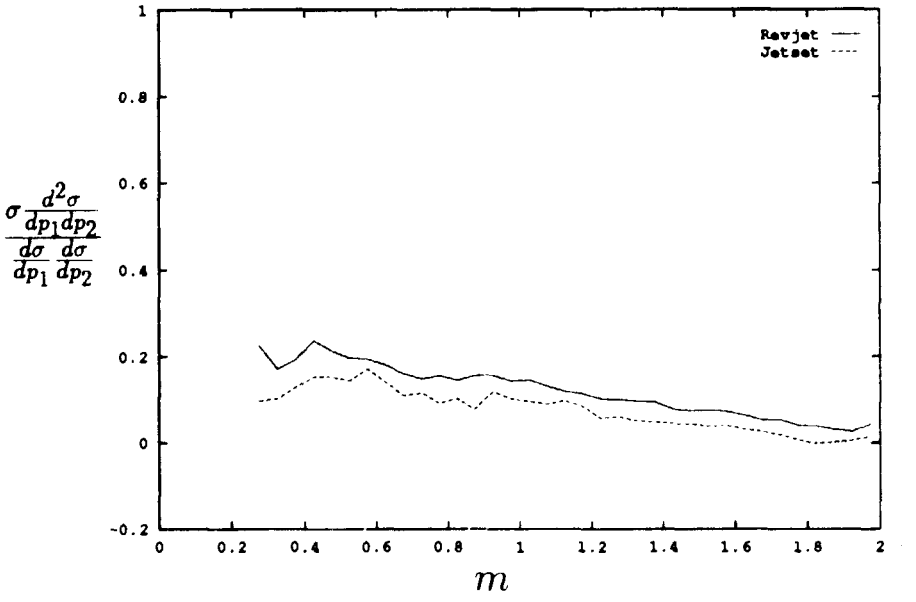

Figure 15: The two-particle correlations between all produced particles in a gluon jet.

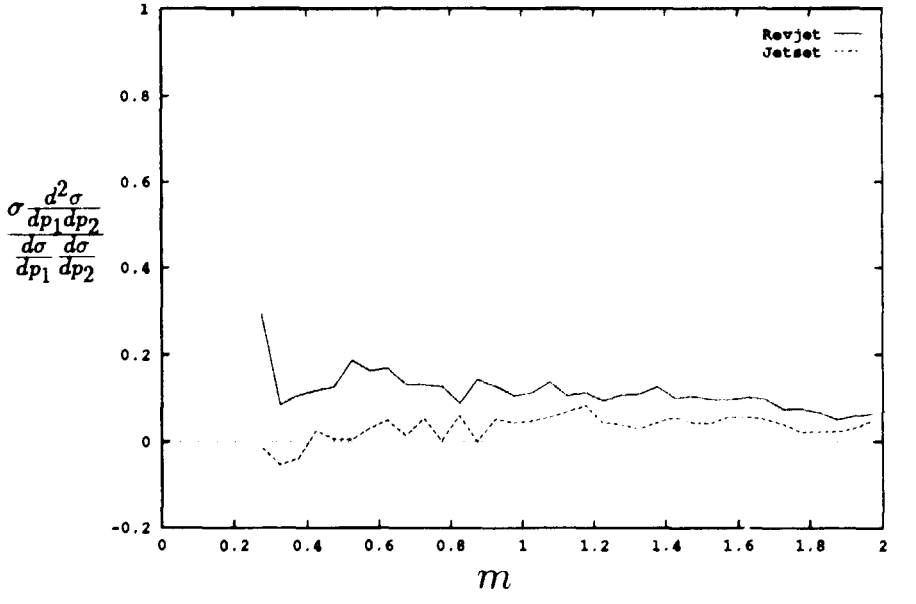

Figure 16: The same as Fig 15 but for the fastest half of the particles.

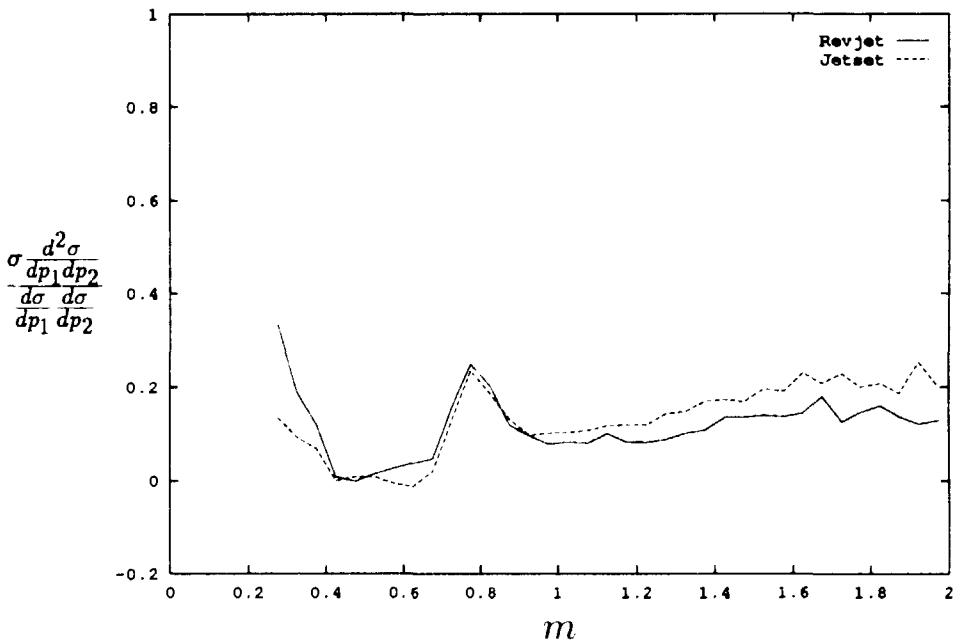

Figure 17: The two-particle correlations for the final state pions after decay.

Inside the gluon jets there are everywhere larger two-particle correlations in mass from the REVJET results compared to JETSET. This is noticeable in Figs 15 describing all the produced particles without any decays. In Fig 16 we present the same results for that half of the particles in a gluon jet which are the fastest. This result also survives at least for the small combined masses also after we have decayed all particles and sample only the pions, Fig 17.

Acknowledgements

We would like to thank G. Gustafson and T. Sjöstrand for valuable discussions.

References

[1] T. Sjöstrand, *Comp. Phys. Comm.* **39** (1986) 347
T. Sjöstrand, M. Bengtsson; ibidem **43** (1987) 367

[2] B. Andersson, P. Dahlqvist, G. Gustafson, *Phys. Lett.* **B214** (1988) 604; *Z. Phys.* **C44** (1989) 455, ibidem 466; *Nucl. Phys.* **B328** (1989) 326

[3] T. Sjöstrand, *Nucl. Phys.* **B248** (1984) 469

[4] B. Andersson, G. Gustafson, B. Söderberg, *Nucl.Phys.* **B264** (1986) 29

[5] Yu.L. Dokshitzer, V.A. Khoze, A.H. Mueller, S.I. Troyan, Basics of Perturbative QCD, Editions Frontiere 1991

[6] A. Nilsson, to be published;

[7] L. Lönnblad, A. Nilsson, *Comp. Phys. Comm.* **71** (1992) 1

[8] L. Lönnblad, Lund Preprint LU TP 89-10 (1989)

[9] Ya.I. Azimov, Yu.L. Dokshitzer, V.A. Khoze, S.I. Troyan, *Phys. Lett.* **B165** (1985) 147
G. Gustafson, U. Pettersson, *Nucl. Phys.* **B306** (1988) 746

[10] M.G. Bowler, *Z. Phys.* **C11** (1981) 169

[11] B. Andersson, G. Gustafson, B. Söderberg, *Z. Phys.* **C20** (1983) 317

[12] B. Andersson, G. Gustafson, A. Nilsson, C. Sjögren, *Z. Phys.* **C49** (1991) 79